

# Biosignature Detection in Exoplanetary Atmospheres Using Monte Carlo Simulations

Undergraduate Research Thesis

Presented in Partial Fulfillment of the Requirements for Graduation *with Research Distinction* in  
Astronomy and Astrophysics in the Undergraduate Colleges of The Ohio State University

By

Michael F. Rothman

Astronomy and Astrophysics Undergraduate Program

The Ohio State University

May 2021

Thesis Defense Committee:

Anil K. Pradhan, Advisor

Sultana N. Nahar

Copyright by Michael Francis Rothman

2021

## Abstract

Development is under way of an exoplanetary atmosphere simulator GEANT4-ExoPlanets (GEANT4-ExoP) based on the multi-purpose Monte Carlo program package GEANT4, which enables modeling transmission of radiation and particles through matter. GEANT4-ExoP will provide a toolkit to model the transmission of host-star radiation through differentiated atmospheric layers using radiative transition data for a plethora of atoms and molecules. GEANT4-ExoP will allow observations to be compared with simulated spectra, demystifying atomic and molecular abundances in exoplanetary atmospheres. We focus on biosignatures such as H, C, N, O, P, and S atoms and molecules comprised of them. The Sun-Earth system will be fully simulated first as a test case with a focus on modeling absorption and emission spectral features. With the data filtered through GEANT4-ExoP, we report Gaussian convolutions of the Kurucz simulated solar irradiance and flux residual spectra. Precise atomic radiative transmissions are calculated using SUPERSTRUCTURE (SS), a program package that computes atomic energies, probabilities, and opacities. Sample results of spectroscopic diagnostic lines for P<sub>xiv</sub> are reported, with their values being compared to NIST values and other published results, ensuring accuracy and precision. Transition probabilities for biosignature molecules are obtained through collaboration with the EXOMoL team at the University of College London. Calculations will be conducted for many atoms and integrated into GEANT4-ExoP following assurance of accuracy. Current work is dedicated to developing the module to generate monochromatic opacity profiles for each atom and molecule. GEANT4-ExoP will

provide a toolkit for the modeling of host-star radiation transmission through exoplanet atmospheres, allowing for assessment of habitability and characterization of biosignature abundances within observations.

To my grandfather, Donald Rothman.

## Acknowledgements

I first would like to thank Dr. Anil Pradhan, my mentor and research advisor. When I applied for SURP I never imagined I would be joining such a tight-knit research group. Working on a project merging biology, astrophysics and atomic physics while also utilizing my skills as a programmer has been both a welcomed challenge and a dream realized. During what has turned out to be one of the most difficult years of my life, you have provided me with a wealth of knowledge, patience and guidance as well as fueling my passion for this field, my research, and my curiosity. Whether it is teaching me atomic theory or giving me life advice, I sincerely appreciate all you have done for me and I am eager to continue this project and working with you.

Next, I would like to thank my second mentor, Dr. Sultana Nahar. When I began this project for SURP, you immediately took me under your wing and taught me atomic theory with Bilal. I still use these lessons you taught me to this day, especially about SUPERSTRUCTURE. I am very thankful for the guidance and encouragement you have given me over the past year, especially towards presenting my work at conferences. You and Anil both have shaped me into the rough beginnings of a scientist, and I am excited to keep working with and learning from you. I am truly grateful.

I would also like to thank Dr. Todd Thompson, Dr. David Weinberg, the Ann S. Tuttle Fund and Dr. Gerald and Ann Newson. The financial support and encouragement given to my SURP class during this pandemic was astonishing. I would not be where I am now without the opportunity you provided to me, nor would this thesis likely have been written. I owe you my gratitude.

Thank you to Miss Anna Voelker, Dr. Wayne Schlingman, Mr. James Johnson and all those who enabled the first ever virtual SURP to come to fruition. The program was a “foot in the door” for me and many others in my class during a time when we were not sure we would get one. Your encouragement, patience, and enthusiasm for our success made all the difference.

I would also like to thank Mr. Bilal Shafique. You have consistently pushed and encouraged me to become a better scientist and a better man. Your drive and passion for physics is inspiring and I know you will accomplish great things. I am blessed to have shared my culture with you and vice-versa during your time in the United States and honored to have you as a friend even though you are again on the other side of the globe.

Thank you to the Ohio Supercomputer Center and the Arts and Sciences Technology Services’ Unity Cluster, both in Columbus, Ohio, for providing a platform to conduct my research.

Finally, thank you to my parents David and Katie Rothman, my siblings MaryKate and Jacob, and the rest of my family and friends. The love, patience and cheering on as I work towards my goals has been truly amazing. I would not be here without all of you, and there are not enough ways to say thank you.

## Table of Contents

<b>Abstract</b> .....	ii
<b>Dedication</b> .....	iv
<b>Acknowledgements</b> .....	v
<b>List of Tables</b> .....	ix
<b>List of Figures</b> .....	x
<b>1. Introduction</b> .....	1
<b>2. Methods</b> .....	3
2.1 Modeling Radiative Transfer .....	3
2.2 Calculating Monochromatic Opacities .....	4
2.3 System Geometry. ....	6
2.4 Creation of Atmospheric Phantom .....	7
2.5 GEANT4-ExoP. ....	7
2.6 Atomic Structure Calculations .....	9
<b>3. Data Acquisition</b> .....	11
3.1 Atomic Data .....	12
3.2 Molecular Data .....	13
<b>4. Conclusion and Future Directions.</b> .....	15



<b>References</b> .....	17
<b>Tables</b> .....	20
<b>Figures</b> .....	21
<b>Appendix A: GEANT4 Installation</b> .....	28
<b>Appendix B: SUPERSTRUCTURE</b> .....	29

## List of Tables

Table 1	Table of energies for H-like phosphorus . . . . .	20
---------	---	----

## List of Figures

Figure 1	Flowchart of GEANT4-ExoP . . . . .	21
Figure 2	The geometry of the stellar flux incident on an exoplanet . . .	22
Figure 3	Solar radiation distribution compared with Black-body Planck function . . . . .	23
Figure 4	Solar radiation spectra plotted as irradiance against air wavelength . . . . .	24
Figure 5	Solar energy received on Earth's surface plotted as residual flux against wavelength . . . . .	25
Figure 6	Predicted diagnostic w, x, y, z lines of He-like phosphorus ( $P_{XIV}$ ) . . . . .	26
Figure 7	Observed w, x, y, z lines of He-like O in Procyon corona . . .	27

# 1. Introduction

Through the hard work of several missions, most notably the Kepler Space Telescope, Spitzer Space Telescope, and TESS, over 4,300 exoplanets have been confirmed (Samara et al., 2021). The natural step, which is now under way, is from discovery to categorization and characterization. The upcoming launch of the James Webb Space Telescope (JWST) in late 2021 will be an excellent way to accomplish this (Deming et al., 2009; Stevenson et al., 2016). Atmosphere detection on rocky exoplanets, a feat few thought possible decades ago, is reported in several cases (Swain et al., 2021; Barclay et al., 2021). Detection of biosignatures in an Earth-like exoplanet atmosphere would be a novel discovery indeed. Presently, Earth is the only planet known to harbor life, and thus it is a prime candidate for study as astronomers peer out towards other rocky worlds. If one understands how the Earth's atmosphere appears when observed from a distant point, detection of potential biosignatures in exoplanet absorption spectra are more easily characterized and confirmed (Westphal & Pradhan, 2018). GEANT4-ExoP, an adaptation to CERN's GEANT4 Monte Carlo package, will simulate the passage of stellar radiation fields through exoplanetary atmospheres and aid the investigation of biosignature abundances.

Due to GEANT4's original design for use in high-energy particle physics, the program package is generally not as accurate in the low-energy regime, below 1000 eV (Westphal & Pradhan, 2018). These lower energies are the primary range in which transmission spectroscopy for astrobiology occurs. For uses in this field, other physics packages were necessary to improve accuracy and performance in the low-energy regime. One such package, GEANT4-DNA (Incerti

et al., 2010), provides vital improvements specifically for the accuracy of water-based interactions. GEANT4 and GEANT4-DNA are the foundations from which GEANT4-ExoP is built from. To peer into absorption spectra and discern chemical constituents, GEANT4-ExoP must contain a significant database of monochromatic opacities for atoms and molecules in the UV, visible and infrared. To do this, we pull from multiple sources.

GEANT4-ExoP will import transition energies and probabilities for atoms and molecules considered biosignatures. This is a non-trivial step. We calculate atomic transition information using SUPERSTRUCTURE (SS) and LS coupling. SS is a FORTRAN program package specializing in calculations of multiconfiguration atomic structure and processing of data, including energies and transition probabilities, for positive ions and neutral atoms (Eissner et al., 1994). For atomic data incorporated into GEANT4-ExoP, we first focus on key atoms like H, C, N, O, P, and S representing those which a significant majority of biosignature molecules are comprised of. Reported in Table 1 is a sampling of transition energies for H-like phosphorus. We obtain transition energy and probability lists for numerous biosignature molecules through collaboration with the EXOMoL project (Tennyson et al., 2016; Tennyson, 2018). Focus is on key biosignature molecules such as O<sub>2</sub>, CO<sub>2</sub>, H<sub>2</sub>O, N<sub>2</sub>, N<sub>2</sub>O, CH<sub>4</sub>, CH<sub>2</sub>Cl, and CH<sub>2</sub>SH (Seager, 2014; Westphal & Pradhan, 2018). Vital biosignatures are those unlikely to be produced through abiotic processes and originate through a secondary metabolism (Sousa-Silva et al., 2018; Seager & Bains, 2015).

## 2. Methods

### 2.1. Modeling Radiative Transfer

We begin with the basic radiative transfer equation for a frequency  $\nu$ :

$$I_\nu = I_o(\nu)e^{-\tau_\nu},$$

where the intensity is a function of the initial intensity  $I_o(\nu)$  and the optical depth  $\tau_\nu$ . The optical depth is

$$\tau_\nu = I\rho\kappa_\nu,$$

where  $I$  is the geometrical depth,  $\rho$  is the density of a given material, and  $\kappa_\nu$  is the monochromatic opacity (see Section 2.2) of the frequency. We will use this formula extensively in GEANT4-ExoP's calculations to model radiative transfer between the multilayer exoplanetary atmosphere and the stellar radiation field incident upon it.

The Monte Carlo method is integral to the simulation of radiation field interactions with the exoplanetary atmosphere. This method is the backbone of GEANT4 simulations and achieves the application of the Monte Carlo method using random number generators (RNGs) (Westphal, 2019). Encounters between light and a particle in GEANT4, for example, uses this method to approximate the probabilistic nature of the interactions. Let one hypothesize a photon with a 20% chance of being absorbed by an atom in the model. Once the photon is incident upon the atom, GEANT4 generates a random number, e.g. 1-10, where if a 1 or 2 is rolled the event occurs. Of course, if any other number is rolled, the event flag is false, and the photon continues traveling through the defined material until it is absorbed or escapes from the substance.

Photoabsorption events for atoms and molecules in GEANT4 are also accompanied by other processes (e.g. ionization events, Einstein A and B decay coefficients) in their utilization of the Monte Carlo method (Westphal, 2019). The opacity and density are the main factors material-wise dictating these interactions and are defined by libraries containing a wealth of information about the composition (mixture or chemical compound) and state (solid, liquid, gas) (Allison et al., 2016; Agostinelli et al., 2003). The reliance on cross sections and opacities to dictate events is thus why there is such an importance on the calculation of monochromatic opacity profiles.

## 2.2. Calculating Monochromatic Opacities

The focus for cross section and opacity calculations is on bound-bound and bound-free interactions.

For bound-bound interactions, the transition between two atomic levels, 1 and 2, for an atomic species X in lower state 1 follow

$$X_1 + h\nu_{12} \rightarrow X_2.$$

For bound-bound interactions, the cross section is

$$\sigma_v^{bb}(1 \rightarrow 2) = \left( \frac{\pi e^2}{m_e c} \right) f_{12} \phi_v ,$$

where  $\phi_v$  is the line profile factor distributing the absorption oscillator strength  $f_{12}$ , defined as

$$f_{12} = \left( \frac{4\pi^2 m_e}{e^2 h} \right) \left( \frac{\nu_{12}}{3g_1} \right) S_{12}.$$

$S_{12}$  is the dipole line strength  $\mathbf{S}_{12} = e|\langle\psi_2||\mathbf{D}||\psi_1\rangle|^2$  and dipole operator  $\mathbf{D} = \sum_i r_i$  (Pradhan & Nahar, 2011).

With these equations we define the bound-bound monochromatic opacity in two ways:

$$\kappa_\nu^{12}(bb) = \left(\frac{\pi e^2}{m_e c}\right) N_1 f_{12} \phi_\nu,$$

$$\kappa_\nu(bb; 1 \rightarrow 2) = N_1 \sigma_\nu(1 \rightarrow 2).$$

For a sufficiently energetic photon incident on an atomic species X, a bound-free transition occurs in which the electron is ionized from bound state b by the process:

$$X_b + h\nu_{b\epsilon} \rightarrow X^+ + e(\epsilon),$$

where  $h\nu_{b\epsilon}$  is the photon energy and  $e(\epsilon)$  is the ejected electron carrying the excess energy  $\epsilon$  (Pradhan & Nahar, 2011).

The photoionization cross section is then expressed as

$$\sigma_\nu(b \rightarrow \epsilon) = \left(\frac{2\pi\nu}{3g_b c}\right) \mathbf{S}(b \rightarrow \epsilon),$$

where  $\mathbf{S}$  now depends on bound state wavefunction  $\psi_b$  and free electron wavefunction  $\psi_\epsilon$ , giving

$$\mathbf{S}(b \rightarrow \epsilon) = |\langle\psi_\epsilon||\mathbf{D}||\psi_b\rangle|^2.$$

Finally, the bound-free monochromatic opacity in terms of the dipole line strength  $\mathbf{S}$  is

$$\kappa_\nu(bf; b \rightarrow \epsilon) = \frac{2\pi\nu N_b}{3g_b c} \mathbf{S}(b \rightarrow \epsilon).$$

All the monochromatic opacities have units of  $\text{cm}^2\text{g}^{-1}$  (Pradhan & Nahar, 2011).



### 2.3. System Geometry

For any planet orbiting at least one host star, the stellar flux that reaches the planet interacts with the atmosphere. This process imprints the spectroscopic features of the atmosphere on the radiation field due to photoabsorption and reemission. When an exoplanet passes between its host star and an observer, a portion of the incident radiation field passes through the atmosphere before reaching the observer. This process is visualized in Figure 2 (Westphal & Pradhan, 2018). This geometry fundamentally is what GEANT4-ExoP will model, allowing the user to simulate the absorption spectra of the atmosphere on the stellar flux.

As a first proof of the capabilities of the application of GEANT4, we model the Earth and Sun. Given the Earth is the only known planet sustaining life, it serves as a trove of information for the search of DNA-based life in other systems. The use of the solar radiation distribution is vital to the simulation. As seen in Figure 3 one cannot approximate the spectrum as a perfect blackbody for the Sun due to the poor fit of the curve to observations (Pradhan & Nahar, 2011). While in the near-infrared to infrared wavelengths the solar spectrum correlates with the black-body function, there exist significant differences in the UV wavelengths. The black-body Planck distribution function defining the energy-wavelength relationship takes the form

$$B_{\lambda}(T_*) = \frac{2hc^2}{\lambda^5} \frac{1}{\exp\left(\frac{hc}{\lambda kT_*}\right) - 1}$$

where  $T_*$  is the radiation temperature of the star ( $T_* = 5770\text{K}$  for the Sun),  $\lambda$  is the wavelength of the photons,  $c$  is the speed of light,  $h$  is Planck's constant, and  $k$  is the Boltzmann constant.

## 2.4. Creation of Atmospheric Phantom

Using existing GEANT4 architecture, we model the planet and its atmosphere using a phantom. The atmospheric layers are defined as their own material and stacked. Each layer material contains a distinct composition (e.g. for Earth case: ~80% N<sub>2</sub>, ~20% O<sub>2</sub> in the stratosphere; mainly free N, O, He in ionosphere<sup>1</sup>) which interacts uniquely with the solar radiation field (Westphal, 2019). The composition of each layer is composed of atoms and molecules, defined in GEANT4-ExoP for those not included in GEANT4 libraries. Flux moves through galactic material, composed of hydrogen at pressure  $3 \times 10^{-18}$  Pa, density  $10^{-25}$  g/cm<sup>3</sup>, and temperature 2.73 K before and after interacting with the multilayer atmospheric phantom (Westphal & Pradhan, 2018). In the Sun-Earth case, we collect the absorption spectrum as if it is an Earth-analog orbiting a Sun-like star (type G2 V,  $T_{eff} = 5770$  K) allowing for an easier transition into the general case once the Sun-Earth case is demonstrated.

## 2.5. GEANT4-ExoP

GEANT4-ExoP builds off CERN’s GEANT4 Monte Carlo program package to determine chemical abundances within the absorption spectra of exoplanetary atmospheres. GEANT4’s main function is to simulate the passage of particles through matter, and its open-source platform allows for users to design a wide range of experiments (Agostinelli et al., 2003). Programmed in C++, GEANT4’s versatility allows it to complete a large variety of tasks with good accuracy and speed. As discussed in the introduction, GEANT4-ExoP will provide an

---

<sup>1</sup> <http://www.naic.edu/~isradar/is/aboutis/composition.html>

additional program package for the simulation of stellar radiation field interactions with orbiting exoplanets. The operation flowchart of GEANT4-ExoP can be seen in Figure 1, and I will provide more detail sequentially.

We first import stellar radiation fields into GEANT4-ExoP. For candidate stars, we look towards stars similar to and cooler than the Sun. G-, K-, and M-type dwarfs are primary candidates in the search of habitable exoplanets due to their lower output in ultraviolet wavelengths and longer lifespans compared to F-type stars.

Once an irradiance spectrum is imported into GEANT4-ExoP, the user defines the planetary structure, including the density, temperature, and atmospheric composition. The atmosphere of the planet is layered in a way analogous to Earth, with emphasis on the composition of the ionosphere. The multilayered approach to the simulated phantom atmosphere allows for more accurate stellar radiation field interactions, producing a more accurate absorption spectrum.

At this point, GEANT4-ExoP references and reads in required atomic and molecular data. GEANT4-ExoP will contain a repository of data for select atoms and molecules, although more data will be added to the database over time to continually improve accuracy. We utilize SUPERSTRUCTURE (SS) to calculate atomic transition data vital for the calculations of photoionization cross sections and consequently monochromatic opacities. We similarly extract molecular transition data from EXOMoL, generating photoionization cross sections and monochromatic opacities with this information as well.

Once calculated for a given configuration, photoionization cross sections  $\sigma_{PI}$  and monochromatic opacities  $K_\nu$  are stored for efficient future utilization. We focus on the bound-bound and bound-free opacities to simplify the calculation, neglecting the inverse bremsstrahlung process.

With this wealth of data, emission spectra are calculated according to inputted stellar radiation fields. The stellar radiation field is propagated through the simulated differentiated atmosphere (phantom), where the irradiance interacts with the atmosphere. This absorption spectrum produced from propagation through the phantom atmosphere (and microscopically, absorption and reemission by the atoms (ions, molecules)) falls incident upon the GEANT4 detection device where the data is collected. The model's absorption and emission spectra are analyzed, determining abundances from line intensities. Data is collected in output files for user convenience before operations cease.

## 2.6 Atomic Structure Calculations

While there are numerous equations and approximations utilized in the calculations for SUPERSTRUCTURE (SS), I will focus on those directly related to work done so far with the package.

The energy levels for a hydrogenic atomic system follow as

$$E = -\frac{Z^2}{n^2} \text{ Ry},$$

for a given charge number  $Z$  and principal quantum number  $n$ . For systems with greater than 1 electron, we must consider the screening effect on the valence electron by the closed shell of core electrons (Pradhan & Nahar, 2011). Thus, we modify the above equation for  $n$  and orbital angular momentum quantum number  $l$  to

$$E(nl) = \frac{z^2}{(n-\mu_l)^2},$$

where the effective charge is  $z = Z - N + 1$  for  $N$  electrons, and quantum defect parameter  $\mu_l$  (Pradhan & Nahar, 2011).

Photo-excitation and de-excitation or bound-bound transitions have transition probability, for frequency  $\nu$ , and energy levels  $i, j$ :

$$P_{ij} = 2\pi \frac{c^2}{h^2 \nu_{ji}^2} |\langle j | \frac{e}{mc} \hat{e} \cdot p e^{ik \cdot r} | i \rangle|^2 \rho(\nu_{ji}),$$

where  $e^{ik \cdot r} = 1 + ik \cdot r + \frac{[ik \cdot r]^2}{2!} + \dots$ ,  $\rho(\nu_{ji})$  is the spatial density of electrons (Nahar, 2020; Nahar, 2021). Each allowed electric dipole transition (E1) also has corresponding oscillator strength

$$f_{ij} = \left[ \frac{E_{ji}}{3g_i} \right] S,$$

for  $S$  as defined in Section 2.2, and corresponding radiative decay rate (Nahar, 2020; Nahar, 2021)

$$A_{ji}(\text{sec}^{-1}) = \left[ 0.8032 \times 10^{10} \frac{E_{ji}^3}{3g_i} \right] S.$$

Selection rules dictate certain forbidden transitions for photo-excitation and de-excitation, listed below (Nahar, 2020; Nahar, 2021):

1. E2: electric quadrupole transitions ( $\Delta J = 0, \pm 1, \pm 2, \pi$  (parity) same)

$$A_{ji}^{E2}(\text{sec}^{-1}) = \left[ 2.6733 \times 10^3 \frac{E_{ij}^5}{g_j} \right] S^{E2}(i, j);$$

2. M1: Magnetic dipole transitions ( $\Delta J = 0, \pm 1, \pi$  (parity) same)

$$A_{ji}^{M1}(\text{sec}^{-1}) = \left[ 3.5644 \times 10^4 \frac{E_{ij}^3}{g_j} \right] S^{M1}(i, j);$$

3. E3: Electric octupole transitions ( $\Delta J = \pm 2, \pm 3, \pi$  (parity) changes)

$$A_{ji}^{E3}(\text{sec}^{-1}) = \left[ 1.2050 \times 10^{-3} \frac{E_{ij}^7}{g_j} \right] S^{E3}(i, j);$$

4. M2: Magnetic quadrupole transitions ( $\Delta J = \pm 2, \pi$  (parity) changes)

$$A_{ji}^{M2}(\text{sec}^{-1}) = \left[ 2.3727 \times 10^{-2} \frac{E_{ij}^5}{g_j} \right] S^{M2}(i, j).$$

Some of these forbidden transitions can be used for observational diagnostic lines. For example, the diagnostic lines of O VII, seen in Figure 7, x and z are the M2 transition from  $1s2p(^3P_2^o) - 1s^2(^1S_0)$  and M1 transition from  $1s2s(^3S_1) - 1s^2(^1S_0)$ , respectively.

### 3. Data Acquisition

Observational or synthetic stellar spectra are inputted into GEANT4-ExoP to create the radiation field. The radiation field is propagated through a galactic medium before and after interactions with the multilayer atmosphere of the phantom. In the Sun-Earth test case, we filter

solar irradiance and flux residual atlases (Kurucz, 2005) through GEANT4 data structures. This simple process, modulated into separate programs to handle each spectrum separately, reads the spectra into GEANT4 vectors before outputting vectors into text files. Raw data can be seen plotted using Matlab in Figures 4a and 5a. This outputted data undergoes a Gaussian convolution with resolution comparable to that of observational data. Convolving the data smooths fine structure transitions unable to be resolved by observational resolutions. Figures 4b and 5b show the smoothed spectra with a comparable resolution of 1 nm. We use `gausswin` to generate the Gaussian, plotting it with the typical methods. Obtaining the spectra back from the program package proves the capabilities of GEANT4 for the lower energy threshold.

### 3.1. Atomic Data

We obtain predicted values of transition energies, opacities, and other vital information for atoms and ions through SUPERSTRUCTURE (SS) calculations. The present focus is on calculations for phosphorus as it is a key component of DNA-based life (Rothman et al., 2020). Given that DNA is the basis of all known life, any stellar system we investigate for evidence of biosignatures must contain a detectable abundance of phosphorus. High priority atoms (ions) for incorporation into GEANT4-ExoP also include H, C, N, O, and S. SS (Appendix B) is used for these calculations in conjunction with the NIST Atomic Spectra Database<sup>2</sup> (NIST) to verify accuracy and precision of theoretical results to NIST-accepted values. A sampling of computed energies for H-like phosphorus is shown in Table 1, and a comparison with accepted NIST

---

<sup>2</sup> [https://physics.nist.gov/PhysRefData/ASD/levels\\_form.html](https://physics.nist.gov/PhysRefData/ASD/levels_form.html)

values shows a maximum error of 0.071%. We verify all computed results with NIST values as well as published results to ensure accuracy and precision to known calculations and observations before importing the data into GEANT4-ExoP. Accuracy is improved through manual tweaking of “a” coefficients within SS. Calculations for neutral phosphorus and all configurations of ionic phosphorus are currently in preparation for publication.

Accuracy is also shown through spectroscopic diagnostic lines. Seen in Figure 6 are the predicted transition probabilities for w, x, y, and z diagnostic lines of He-like phosphorus, P<sub>XIV</sub>. This is an example of x-ray lines whose ratios yield accurate temperature and density diagnostics. A key point in Figure 6 is the lack of line broadening since these lines are predicted. Observations of diagnostic lines, such as those of high-temperature He-like oxygen plasma composing Procyon’s corona seen in Figure 7 (Pradhan & Nahar, 2011), are significantly widened due to density and temperature. Similar effects would be seen through observations of P<sub>XIV</sub> diagnostic lines.

### 3.2. Molecular Data

GEANT4-ExoP’s ability to determine biosignature abundances is heavily dependent on the molecular monochromatic opacity database our group can compile. While biospheres are dependent on dominant molecules such as H<sub>2</sub>O, CO<sub>2</sub>, O<sub>2</sub>, and CH<sub>4</sub>, there are over 16,400 molecules potentially of interest as biosignatures (Sousa-Silva, 2018). Of the roughly 16,400 molecules, only approximately 600 in the literature contain spectral information and a few percentages of those have spectral information considered highly accurate (Sousa-Silva, 2018).



Many of these volatile molecular species may accumulate in a planetary atmosphere and contribute, at least faintly, to the biosphere in a manner such that the species is detectable (Sousa-Silva, 2020). Important species to consider are those that contribute to Earth’s redox disequilibrium, as these molecules would react and neutralize on relatively fast timescales in the absence of life (Grenfell, 2018). GEANT4-ExoP will be equipped first with the molecular spectral information for O<sub>2</sub>, CO<sub>2</sub>, H<sub>2</sub>O, N<sub>2</sub>, N<sub>2</sub>O, CH<sub>4</sub>, CH<sub>2</sub>Cl, and CH<sub>2</sub>SH (Westphal & Pradhan, 2018) as they are perhaps the most studied molecules (especially H<sub>2</sub>O, CH<sub>4</sub>, and CO<sub>2</sub>) with broad wavelength coverage.

We look towards several projects to obtain molecular spectral information for integration into GEANT4-ExoP’s database. Collaboration with EXOMoL (Tennyson et al., 2016; Tennyson, 2018) gives access to transition energies and probabilities for a plethora of volatile molecules, including extensive lists for H<sub>2</sub>O, CO<sub>2</sub>, CH<sub>4</sub>, and many more. We similarly are considering sources such as ATMOS (Sousa-Silva et al., 2018), HITRAN (Gordon et al., 2017), HELIOS-K (Grimm & Heng, 2015), and others although determinations will be made at a later date.

While we consider all three types of molecular transitions on a case-by-case basis, the focus is on electronic rather than rovibrational transitions. This is due to electronic transitions generally dominating absorption and emission in the spectral range of interest: 1,000 – 10,000 Å. From EXOMoL, while we have the transition probabilities for a given molecule, we must use the given molecular level IDs and corresponding energies to calculate the wavelength for each transition probability. To accomplish this, vectors of level IDs and energies for each level ID are stored. Vectors of the level IDs for the transitions are stored and read, the difference in energies

being calculated for each transition and thus paired with its corresponding transition probability. Wavelengths for each transition probability are then calculated using

$$\lambda = \frac{hc}{E}$$

where  $c$  is the speed of light and  $h$  is the Planck constant. These two vectors (calculated transition wavelengths and transition probabilities) are then stored for use in the calculation of a monochromatic opacity profile for the molecule.

## 4. Conclusion and Future Directions

Much progress has been made in the development of GEANT4-ExoP, including proof of concept with importing, filtering, and exporting solar irradiance and residual flux spectra. Work has just begun, however, and we are currently beginning the development of the monochromatic opacity profile module. This module will generate the profile for a given atom (ion, molecule) and store it in a repository, its file linked to the individual class associated with the atom (ion, molecule). We use the methods described in Section 2.2 to calculate the monochromatic opacity profile. During this time, we are also calculating lists of atomic (ionic) transition energies and probabilities using SUPERSTRUCTURE and searching EXOMoL and other molecular spectral databases for biosignature molecules with spectral information in the range required. Code for the calculation of transition wavelength lists is also well into development. These lists will be integrated into GEANT4-ExoP once completed. Following the completion of these modules, building up the repository will be vital and will be done in tandem with the development of the

ionospheric cross section molecule (Figure 1) and developing the actual GEANT4 simulation itself.

The largest proof once modules are assembled is modeling once again the Sun-Earth system. This time we will import the irradiance spectrum but now define the different atmospheric layers of the Earth using defined molecules, atoms, and ions from GEANT4-ExoP's repository. We create a multilayer atmospheric phantom and simulate through it (and a galactic medium) the solar radiation field prior to incidence upon a GEANT4 detector. This geometry ensures we receive an absorption spectrum from the detector identical to observations by viewing the Sun-Earth system as if it is a distant star-exoplanet system. Once proven, our group will begin GEANT4-ExoP simulations for other stellar systems. High probability targets for simulation are those systems in publication suggested for investigation by observations, especially those ranked for investigation by JWST (Fortenbach & Dressing, 2020; Trifnov et al., 2021). While the Sun-Earth case will enable GEANT4-ExoP to be stress-tested and accuracies determined and tweaked, we will use every simulation to tweak the system and improve it. GEANT4-ExoP will be a vital toolkit to determining the chemical abundances of exoplanetary atmospheres.

## References

- Agostinelli, S., Allison, J., Amako, K., Apostolakis, J., Araujo, H., ... Zschesche, D. (2003). GEANT4 - A simulation toolkit. *Nucl. Instruments Methods Phys. Res. Sect. A Accel. Spectrometers, Detect. Assoc. Equip.*, 506(3), 250-303. [https://doi.org/10.1016/S0168-9002\(03\)01368-8](https://doi.org/10.1016/S0168-9002(03)01368-8)
- Allen, C. W. (1976). *Astrophysical Quantities* (3rd ed.). The Athlone Press, University of London.
- Allison, J., Amako, K., Apostolakis, J., Arce, P., Asai, M., ... Yoshida, H. (2016). Recent developments in Geant4. *Nucl. Instruments Methods Phys. Res. Sect. A Accel. Spectrometers, Detect. Assoc. Equip.*, 835(1), 186-225. <https://doi.org/10.1016/j.nima.2016.06.125>
- Barclay, T., Brande, J., Colon, K., Damiano, M., Hedges, C., Hu, R., ... team, L. 98-59. (2021). A tentative detection of a potentially rocky exoplanet's atmosphere from spectral features. *Bulletin of the AAS*, 53(1). Retrieved from <https://baas.aas.org/pub/2021n1i302p08>
- Deming, D., Seager, S., Winn, J., Miller-Ricci, E., Clampin, M., Lindler, D., ... Ennico, K. (2009). Discovery and Characterization of Transiting Super Earths Using an All-Sky Transit Survey and Follow-up by the James Webb Space Telescope. *Publications of the Astronomical Society of the Pacific*, 121(883), 952–967. <https://doi.org/10.1086/605913>
- Eissner, W., Jones, M., & Nussbaumer, H. (1974). Techniques for the calculation of atomic structures and radiative data including relativistic corrections. *Computer Physics Communications*, 8(4), 270–306. [https://doi.org/10.1016/0010-4655\(74\)90019-8](https://doi.org/10.1016/0010-4655(74)90019-8)
- Eissner, W., Jones, M., & Storey, P. (1994). SUPERSTRUCTURE — paper II. incomplete draft.
- Fortenbach, C. D., & Dressing, C. D. (2020). A Framework For Optimizing Exoplanet Target Selection For The James Webb Space Telescope. *Publications of the Astronomical Society of the Pacific*, 132(1011), 054501. <https://doi.org/10.1088/1538-3873/ab70da>
- Gordon, I.E., Rothman, L. S., Hill, C., Kochanov, R.V., Tan, Y., ... Zak, E. J. (2017). The HITRAN2016 molecular spectroscopic database. *Journal of Quantitative Spectroscopy and Radiative Transfer*, 203, 3-69. <https://doi.org/10.1016/j.jqsrt.2017.06.038>
- Grenfell, J. L. (2018). Atmospheric Biosignatures. *Handbook of Exoplanets*, 3159–3172. [https://doi.org/10.1007/978-3-319-55333-7\\_68](https://doi.org/10.1007/978-3-319-55333-7_68)

- Grimm, S. L., & Heng, K. (2015). HELIOS-K: AN ULTRAFast, OPEN-SOURCE OPACITY CALCULATOR FOR RADIATIVE TRANSFER. *The Astrophysical Journal*, 808(2), 182. <https://doi.org/10.1088/0004-637x/808/2/182>
- Incerti, S., Ivanchenko, A., Karamitros, M., Mantero, A., Moretto, P., Tran, H. N., ... Zacharatou, C. (2010). Comparison of GEANT4 very low energy cross section models with experimental data in water. *Medical Physics*, 37(9), 4692–4708. <https://doi.org/10.1118/1.3476457>
- Kurucz, R.L. (2005, Jun. 15-16). *High resolution irradiance spectrum from 300 to 1000 nm*. AFRL Transmission Meeting, Lexington, MA, United States.
- Nahar, S. N. (2020, May-Jun.). *ATOMIC STRUCTURE AND TRANSITIONS: THEORY AND USE OF SUPERSTRUCTURE PROGRAM* [Lecture series]. Computational Workshop, Columbus, OH, United States (Virtual).
- Nahar, S., Shafique, B., Rothman, M., & Naghma, R. (2020, Oct. 16–17). *Abstract: F03.00001: Xray to far infrared spectrum of phosphorus for astrophysical modeling* [Conference session]. APS Ohio Section Fall 2020 Meeting., Virtual.
- Nahar, S. N. (2021, Feb. 5-7). *GRAVITATIONAL WAVES, MERGER OF NEUTRON STARS, BLACK HOLES, AND HEAVY ELEMENTS* [Conference session]. Bangladesh Physical Society, International e-Conference on Physics, Virtual.
- Ness, J.-U., Mewe, R., Schmitt, J. H., Raassen, A. J., Porquet, D., Kaastra, J. S., ... Predehl, P. (2001). Helium-like triplet density diagnostics. *Astronomy & Astrophysics*, 367(1), 282–296. <https://doi.org/10.1051/0004-6361:20000419>
- Pradhan, A. K., & Nahar, S. N. (2011). *Atomic astrophysics and spectroscopy*. Cambridge University Press.
- Rothman, M., Pradhan, A., Nahar, S.N., & Shafique, B. (2020, Jul. 28). *Simulating Spectra of Exoplanetary Atmospheres: Calculating Transmission Energies and Opacities* [Symposium presentation]. OSU Department of Astronomy Summer Undergraduate Research Program Symposium, Columbus, OH, United States (Virtual).
- Samara, E., Patsourakos, S., & Georgoulis, M. K. (2021). A Readily Implemented Atmosphere Sustainability Constraint for Terrestrial Exoplanets Orbiting Magnetically Active Stars. *The Astrophysical Journal Letters*, 909(1). <https://doi.org/10.3847/2041-8213/abe416>
- Seager, S. (2014). The future of spectroscopic life detection on exoplanets. *Proceedings of the National Academy of Sciences*, 111(35), 12634–12640. <https://doi.org/10.1073/pnas.1304213111>

- Seager, S., & Bains, W. (2015). The search for signs of life on exoplanets at the interface of chemistry and planetary science. *Science Advances*, 1(2).  
<https://doi.org/10.1126/sciadv.1500047>
- Sousa-Silva, C., Seager, S., Ranjan, S., Petkowski, J. J., Zhan, Z., Hu, R., & Bains, W. (2020). Phosphine as a Biosignature Gas in Exoplanet Atmospheres. *Astrobiology*, 20(2), 235–268.  
<https://doi.org/10.1089/ast.2018.1954>
- Sousa-Silva, C., Petkowski, J. J., & Seager, S. (2018). ATMOS: Towards Resolving Ambiguities in the Spectroscopic Detection of Life. In C. Mendoza, S. Turck-Chiéze, & J. Colgan (Eds.), *Workshop on Astrophysical Opacities* (Vol. 515, Ser. ASP Conference Series, pp. 241–248). Kalamazoo, MI; Astronomical Society of the Pacific.
- Stevenson, K. B., Lewis, N. K., Bean, J. L., Beichman, C., Fraine, J., ... Wakeford, H. (2016). Transiting exoplanet studies and community targets for JWST's Early Release Science Program. *Publications of the Astronomical Society of the Pacific*, 128(967).  
<https://doi.org/10.1088/1538-3873/128/967/094401>
- Swain, M. R., Estrela, R., Roudier, G. M., Sotin, C., Rimmer, P. B., Valio, A., ... Zellem, R. T. (2021). Detection of an Atmosphere on a Rocky Exoplanet. *The Astronomical Journal*, 161(5), 213. <https://doi.org/10.3847/1538-3881/abe879>
- Tennyson, J., Yurchenko, S. N., Al-Refaie, A. F., Barton, E. J., Chubb, K. L., Coles, P. A., ... Zak, E. (2016). The ExoMol database: Molecular line lists for exoplanet and other hot atmospheres. *Journal of Molecular Spectroscopy*, 327, 73–94.  
<https://doi.org/10.1016/j.jms.2016.05.002>
- Tennyson, J. (2018). The ExoMol Project: Molecular Opacity Calculations at University College London. In C. Mendoza, S. Turck-Chiéze, & J. Colgan (Eds.), *Workshop on Astrophysical Opacities* (Vol. 515, Ser. ASP Conference Series, pp. 137-144). Kalamazoo, MI; Astronomical Society of the Pacific.
- Trifonov, T., Caballero, J. A., Morales, J. C., Seifahrt, A., Ribas, I., ... Winn, J. N. (2021). A nearby transiting rocky exoplanet that is suitable for atmospheric investigation. *Science*, 371(6533), 1038-1041. <https://doi.org/10.1126/science.abd7645>
- Westphal, M. (2019). *Investigation of low energy, alternative X-ray sources and their interactions with multi-Z materials for theranostics*. (Electronic Thesis or Dissertation). Retrieved from <https://etd.ohiolink.edu/>
- Westphal, M., & Pradhan, A. (2018). Monte Carlo Simulations of Biophysical Factors for Viability of Life in Exoplanetary Atmospheres. In C. Mendoza, S. Turck-Chiéze, & J. Colgan (Eds.), *Workshop on Astrophysical Opacities* (Vol. 515, Ser. ASP Conference Series, pp. 249-252). Kalamazoo, MI; Astronomical Society of the Pacific.

K Level	Spectroscopic Notation	SS Energy (Ry)	NIST Energy (Ry)	% Error	
1	$1S_0$	$1s^2$	0	0	-
2	$3S_1$	$1s2s$	156.263	156.153	0.070
3	$3P^0_0$	$1s2p$	157.328	157.273	0.035
4	$3P^0_1$	$1s2p$	157.372	157.295	0.049
5	$3P^0_2$	$1s2p$	157.425	157.384	0.026
6	$1S_0$	$1s2s$	157.472	157.365	0.068
7	$1P^0_1$	$1s2p$	158.313	158.201	0.071
8	$3S_1$	$1s3s$	184.822	184.724	0.053
9	$3P^0_0$	$1s3p$	185.121	185.032	0.048
10	$3P^0_1$	$1s3p$	185.134	185.039	0.051
11	$3P^0_2$	$1s3p$	185.162	185.065	0.052
12	$1S_0$	$1s3s$	185.125	185.044	0.044
13	$3D_1$	$1s3d$	185.331	185.236	0.051
14	$3D_2$	$1s3d$	185.334	185.236	0.053
15	$3D_3$	$1s3d$	185.345	185.247	0.053
16	$1D_2$	$1s3d$	185.352	185.255	0.052
17	$1P^0_1$	$1s3p$	185.393	185.288	0.057
18	$3S_1$	$1s4s$	194.664	194.564	0.051
19	$3P^0_0$	$1s4p$	194.787	194.692	0.049
20	$3P^0_1$	$1s4p$	194.791	194.694	0.050
21	$3P^0_2$	$1s4p$	194.803	194.706	0.050
22	$1S_0$	$1s4s$	194.792	194.694	0.050
23	$3D_1$	$1s4d$	194.872	194.776	0.049
24	$3D_2$	$1s4d$	194.873	194.776	0.050
25	$3D_3$	$1s4d$	194.878	194.780	0.050
26	$1D_2$	$1s4d$	194.882	194.784	0.050
27	$3F^0_2$	$1s4f$	194.881	194.786	0.049
28	$3F^0_4$	$1s4f$	194.881	194.786	0.049
29	$3F^0_3$	$1s4f$	194.884	194.786	0.050
30	$1F^0_3$	$1s4f$	194.884	194.786	0.050
31	$1P^0_1$	$1s4p$	194.897	194.797	0.051
32	$1S_0$	$2s^2$	323.626	323.486	0.043
33	$3P^0_0$	$2s2p$	323.882	323.743	0.043
34	$3P^0_1$	$2s2p$	323.928	323.790	0.043
35	$3P^0_2$	$2s2p$	324.030	323.901	0.040
36	$3P_0$	$2p^2$	324.888	324.766	0.038
37	$3P_1$	$2p^2$	324.940	324.824	0.036
38	$3P_2$	$2p^2$	325.030	324.913	0.036
39	$1D_2$	$2p^2$	325.582	325.428	0.047

Table 1. Table of energies for H-like phosphorus. Comparison of SUPERSTRUCTURE energies (Ry) calculated to accepted NIST energies and the percentage difference between them.

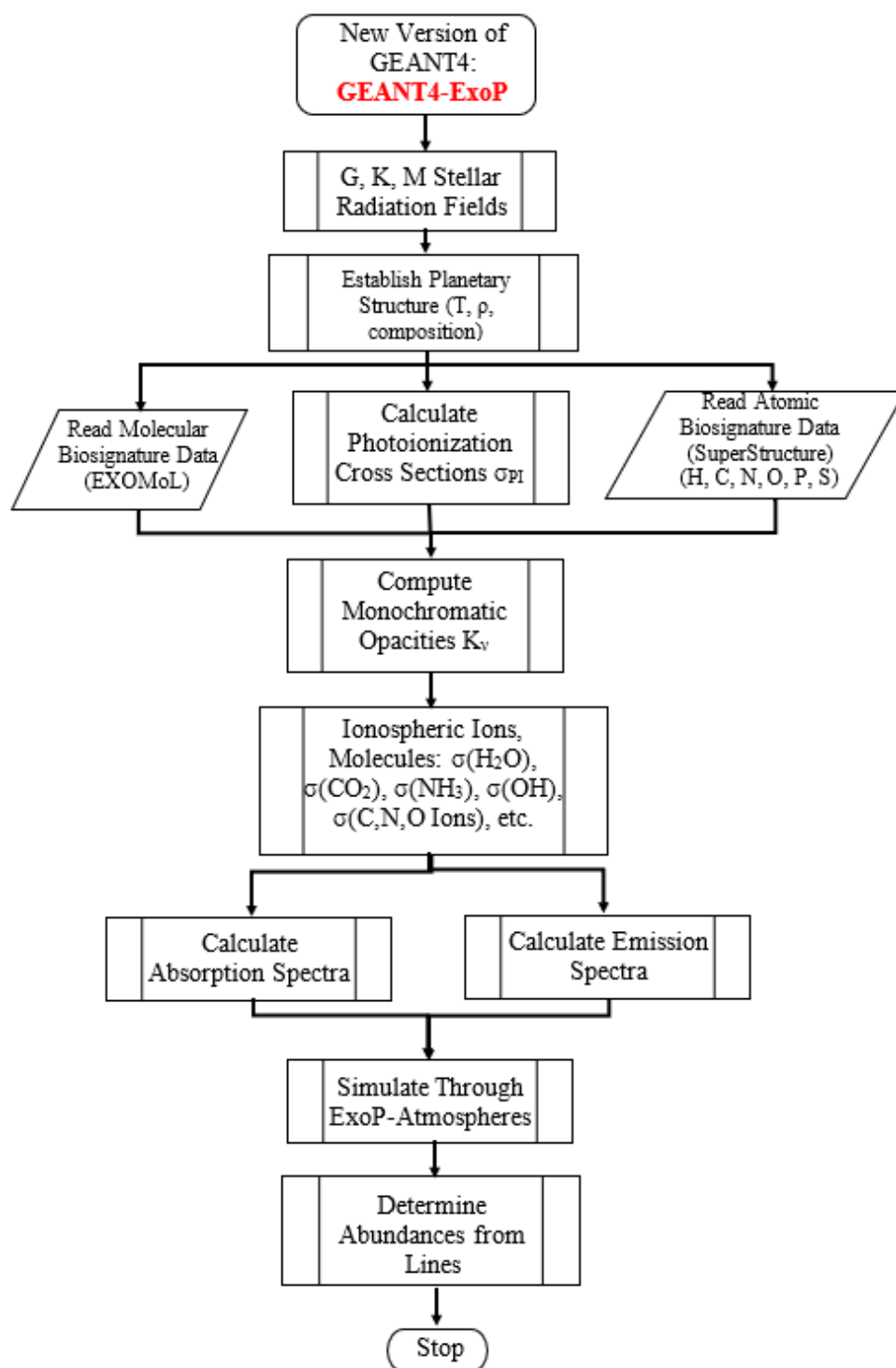


Figure 1. Flowchart of GEANT4-ExoP.



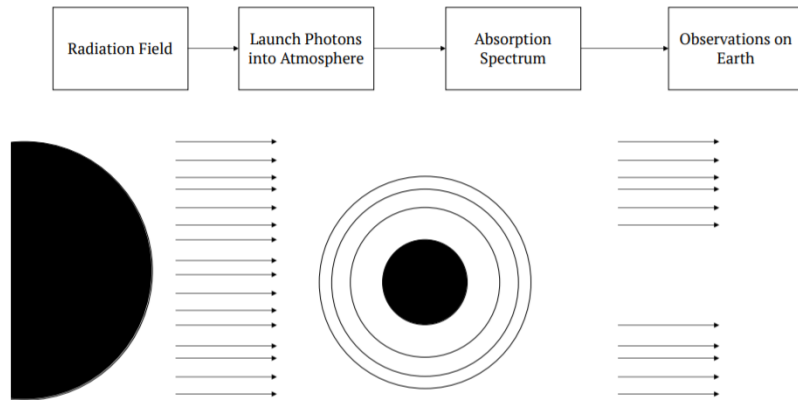


Figure 2. The geometry of the stellar flux incident on an exoplanet. The starlight interacts with the atomic and molecular gases composing the exoplanet atmosphere. The radiation field and produced absorption spectrum pass through GEANT4 vacuum material before reaching the observer (Earth). (Westphal & Pradhan, 2018)

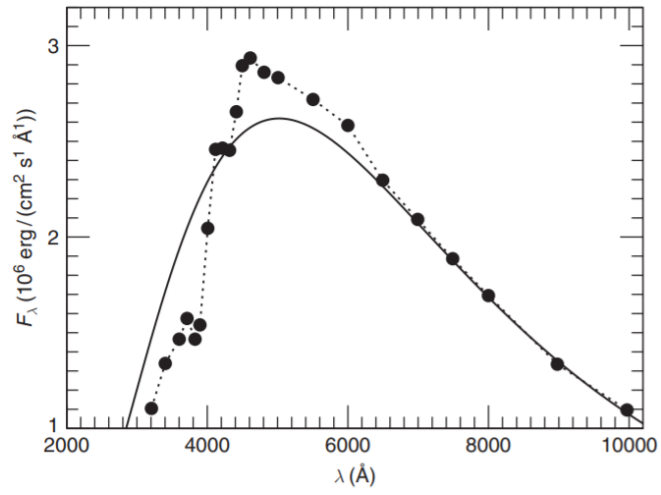


Figure 3. Solar radiation distribution (dashed curve with data points) compared with black-body Planck function (solid line) at  $T_{eff} = 5770$  K. (Allen, 1976)

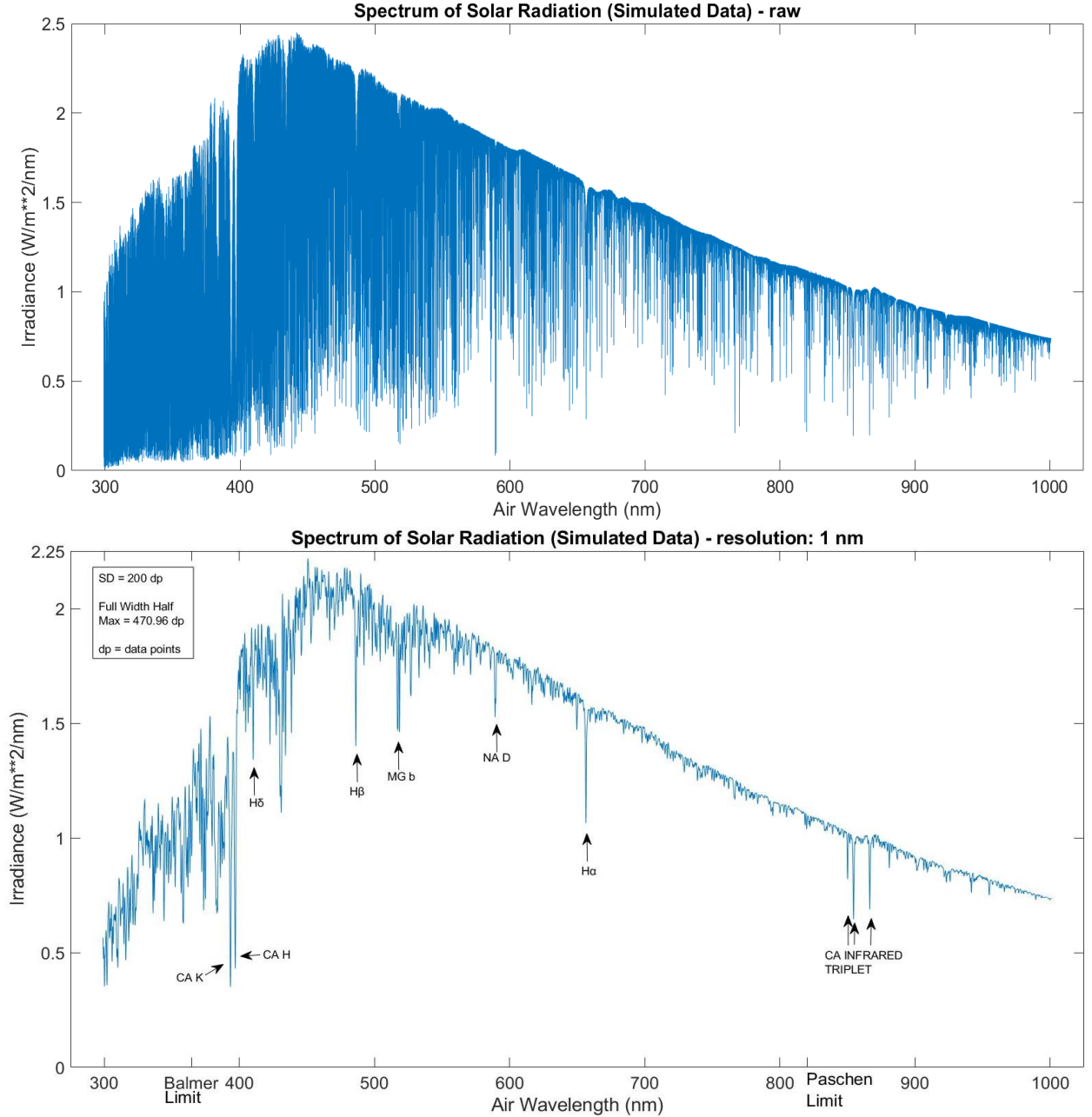


Figure 4(a) and (b). Solar radiation spectra plotted as irradiance against air wavelength. Peak wavelength is  $\sim 450$  nm as expected. Top panel: Figure 3a, the raw data (Kurucz, 2005) simulated for the irradiance field of the Sun. Noise produced by the inclusion of fine structure transitions which would not be observed by observational resolutions. Bottom panel: Figure 3b, the raw data is convoluted using a Gaussian to a resolution of 1 nm. Smoothing the data preserves key features labeled such as the H $\alpha$  line and the calcium infrared triplet.

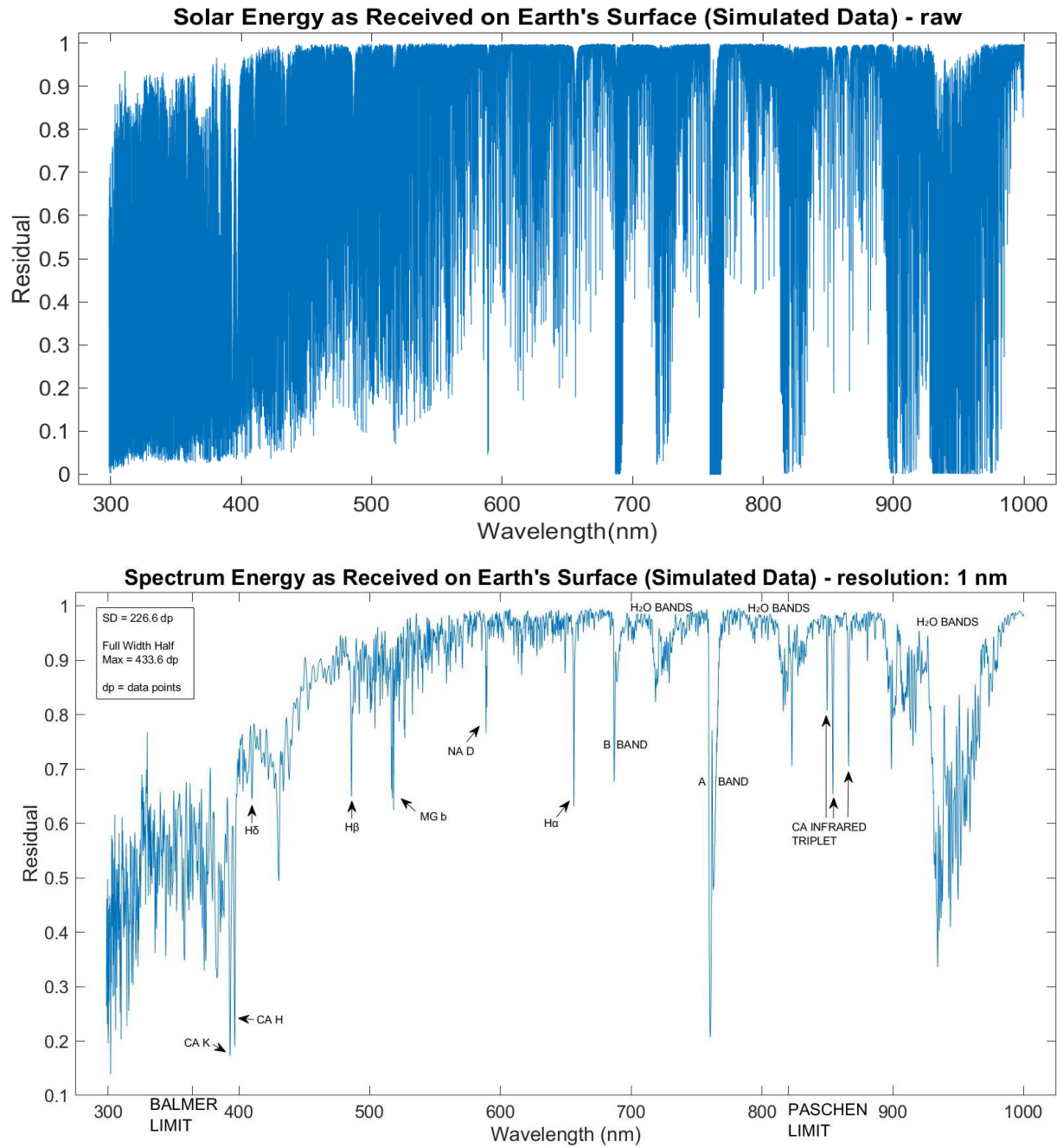


Figure 5(a) and (b). Solar energy received on Earth's surface plotted as residual flux against wavelength. Top panel: Figure 5a, the raw data (Kurucz, 2005) simulated for the residual flux. Noise produced by the inclusion of fine structure transitions which would not be observed by observational resolutions. Bottom panel: Figure 5b, the raw data is convolved using a Gaussian to a resolution of 1 nm. Smoothing the data preserves key features labeled such as the H $\alpha$  line and the infrared H $_2$ O bands.

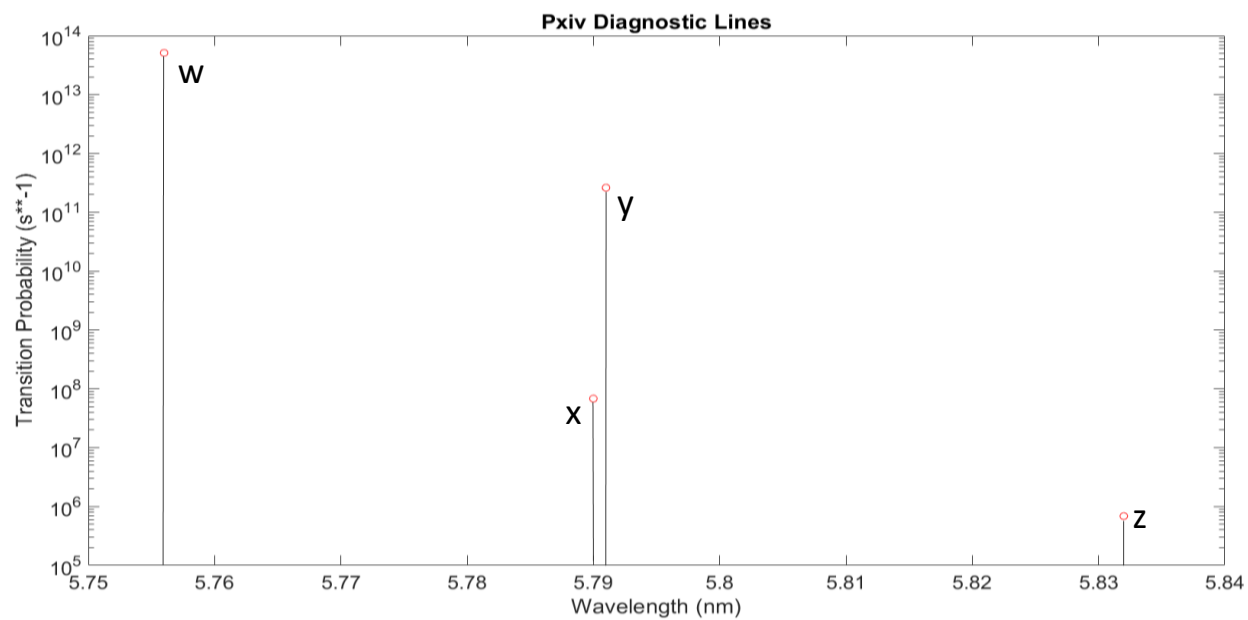


Figure 6. Predicted diagnostic w, x, y, z lines of He-like phosphorus (Pxiv).  
(Nahar, Shafique, Rothman & Naghma, 2020)

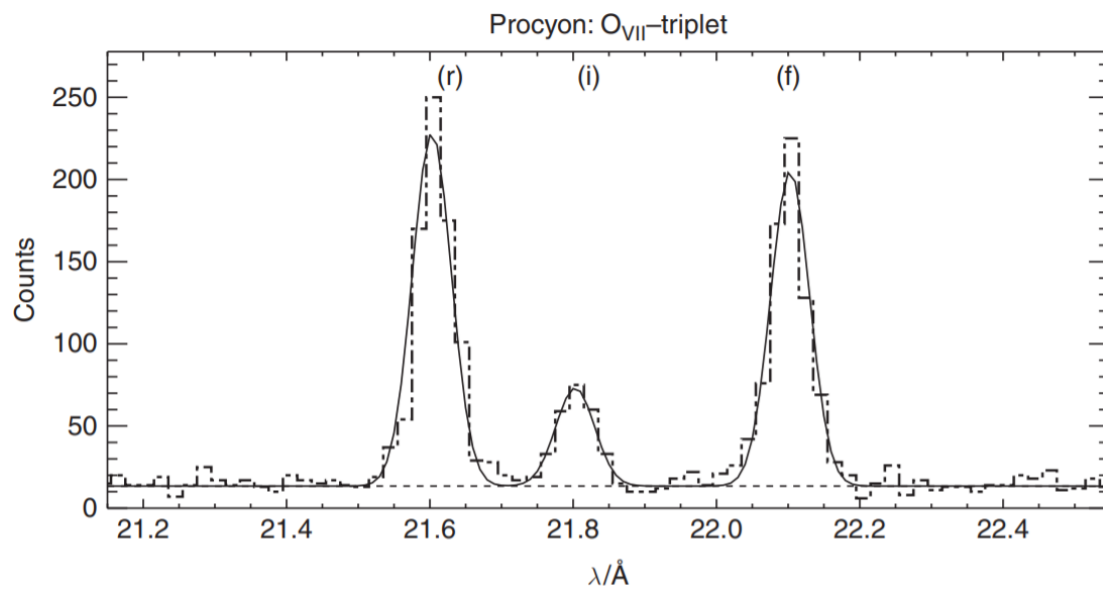


Figure 7. Observed w, x, y, z lines of He-like O in Procyan corona broadened by plasma density and temperature. (Ness et al., 2001, reproduced by permission)

## Appendix A: GEANT4 Installation

The best possible source for direction on installing GEANT4 is CERN's own guide on installation. I link this installation guide below. My recommendation is installing GEANT4 on a Windows system is installing the Unix on the Linux subsystem for Windows. The Linux platform makes working with the program significantly easier. One will follow the tutorial page by page, but much of the installation can be found under "Building and Installing from Source".

<https://geant4-userdoc.web.cern.ch/UsersGuides/InstallationGuide/html/gettingstarted.html>

Once GEANT4 is built, there are numerous examples which are useful for one to use to understand the inner workings of the program package. Examples TestEM11 and TestEM5 are useful to learn modification of G4 materials.

## Appendix B: SUPERSTRUCTURE

In this Appendix, I offer several links to presentations given by Dr. Sultana N. Nahar on SUPERSTRUCTURE (SS) background, set up, and use. Everything one should need to understand and run the program package can be found in these documents.

Computational Workshop (contains links to many different presentations as well as download links to all SS files necessary for beginning):

<http://www.astronomy.ohio-state.edu/~nahar/teaching.html#program>

Under i) Atomic structure calculations using code SUPERSTRUCTURE (SS), the presentation “ATOMIC STRUCTURE AND TRANSITIONS: THEORY” (link below) is essential to understanding the atomic physics behind SS:

<http://www.astronomy.ohio-state.edu/~nahar/research/theo-atomstruct-trans.pdf>

One will also find Dr. Nahar’s presentation “SuperStructureII.pdf” very useful, as this gives a more detailed background to SS. Lastly, “USING SUPERSTRUCTURE PROGRAM” will be vital to first running of the program and contains all the step-by-step information necessary for running SS.

Tips for Use:

- Create a separate folder for each atom or ion one is running SS for. This separates each input file, allowing one to reference the inputs later without losing them.



In Linux, using `mkdir [directory name]` will create a new directory named `[directory name]` in the current directory.

Then, using `cp -R [source directory] [dest directory]` will copy all files from one directory to one's new directory.

- Name files after whatever ion one is working on. For example, "ssin.p13".